EVIDENT | OLYMPUS

# THESE ARE NOT FIREWORKS

This is a single colony of Gloeotrichia captured using a 10X X Line objective.

IMAGE: © HAKAN KVARNSTROM

## See the truth with X Line™ objectives.

Scan the code to discover more.


X LINE

Contact your local sales representative or visit **olympus-lifescience.com/this-is-xline** to learn more.

Received: 23 May 2022 | Revised: 1 September 2022 | Accepted: 13 September 2022

DOI: 10.1111/jmi.13143

Journal of Microscopy RMS

THEMED ISSUE ARTICLE

# Designing chromatic optical retarder stacks for segmented next-generation easySTED phase plates

**Johann Engelhardt**[1] | **Beatrice Ellerhoff**[1] | **Clara-Marie Gürth**[1] | **Steffen J. Sahl**[2] | **Stefan W. Hell**[1,2]

[1]Department of Optical Nanoscopy, Max Planck Institute for Medical Research, Heidelberg, Germany

[2]Department of NanoBiophotonics, Max Planck Institute for Multidisciplinary Sciences, Göttingen, Germany

**Correspondence**
Stefan W. Hell, Max Planck Institute for Multidisciplinary Sciences, Department of NanoBiophotonics, Fassberg Campus, Am Fassberg 11, 37077 Göttingen, Germany.
Email: stefan.hell@mpinat.mpg.de

Present address
Beatrice Ellerhoff, Department of Physics, University of Tübingen, Tübingen, Germany.

**Abstract**

Fluorescence nanoscopy methods based on the RESOLFT principle, such as beam-scanning STED nanoscopy, require the co-alignment of optical beams for molecular state (on/off) switching and fluorescence excitation. The complexity and stability of the beam alignment can be drastically simplified and improved by using a single-mode fibre as the sole light source for all required laser beams. This in turn then requires a chromatic optical element for shaping the off-switching beam into a focal-plane donut while simultaneously leaving the focal intensity distributions at other wavelengths shaped as regular focal spots. Here we describe novel designs of such so-called 'easySTED phase plates' and provide a rationale how to find the desired spectral signature for combinations of multiple wavelengths.

KEYWORDS

fluorescence nanoscopy, intensity minimum, phase plate, polarisation, RESOLFT, STED

## 1 | INTRODUCTION

As a convenient, practical implementation of the STED concept for fluorescence nanoscopy,[1] the easySTED principle was first described by Reuss et al.[2] in 2010. In such a STED microscope (Figure 1), the beams of a set of laser sources are merged and coupled into a single-mode fibre, to provide a single diffraction-limited light source for the scanning microscope. A chromatic phase plate, mounted in the excitation beam path or directly behind the microscope objective, shapes the STED beam into a donut with a central intensity zero at the focus, while the excitation beam remains spot-shaped.[3] The subsequent discussion herein of the chromatic design of easySTED phase plates is formulated in the context of STED nanoscopy, but it obviously applies also to many other optical methods requiring a dedicated spectral behaviour – especially, of course, other RESOLFT methods.[1] Mounting the phase plate directly behind the microscope objective is actually preferable for the beam-shaping device, as this location is very close to the pupil of the objective lens and there are no more optical elements in the illumination beam path which may influence the polarisation state of the beam segments prepared by the chromatic segmented phase plate.

Figure 2A shows a segmented phase plate consisting of four low-order half-wave retarders. The fast axes of the retarders are rotated with respect to each other such that at the design wavelength (of the STED light) the field components $E_x$ and $E_y$ become opposing from opposing segments. These field components therefore cancel each

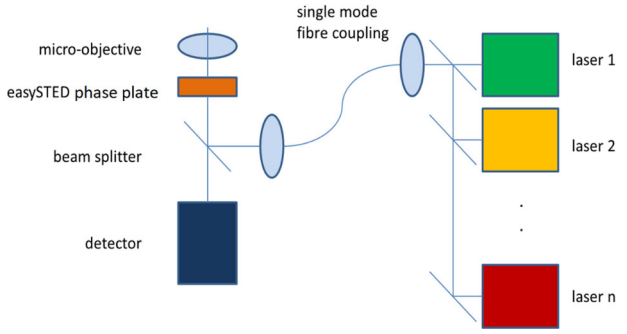


**FIGURE 1** In an easySTED[2] optical setup the laser beams 1…*n* are merged and coupled into a single-mode fibre. The fibre output serves as a single diffraction-limited light source for the scanning microscope for all wavelengths, whose beams are therefore perfectly co-aligned. The scanning microscope is turned into a STED microscope by adding a segmented chromatic 'easySTED' phase plate containing low-order birefringent retarders. The donut-shaped STED beam de-excites fluorophores surrounding the common focal point such that only fluorophores close to the focal point can emit fluorescence photons which are registered by the detector.[1]

other at the focal point, and a donut-shaped intensity pattern is formed in the focal region for light at the STED wavelength. Since the phase retardation is continuously increasing with decreasing wavelength, only distinct wavelengths form exactly a donut with a zero of intensity at the centre. These are the wavelengths for which it acts exactly as a half-wave retarder. At certain shorter wavelengths where the segments become full-wave retarders, the focused beam becomes spot-shaped. This behaviour can be described by a quality function (Figure 2B), to be defined more generally further down in Equation (9). This function is essentially the normalised transmission of a phase plate segment placed at 45° between two linear polarisers. Figure 2C shows the focal intensity distributions for different wavelengths, loosely called point spread functions (PSF), in 10-nm steps. For the example shown, a perfect donut is formed at 775 nm, which is a common STED wavelength. A perfect spot is found close to 650 nm, which is employed for fluorescence excitation.

While the design for the STED wavelength is critical, a less perfect excitation spot does not notably affect the system performance. Calculating the PSF using the theory by Richards and Wolf[4] and including the rate equations for the fluorescence and stimulated emission processes shows that, at ~30 nm resolution, the signal loss is approximately 50% if the central minimum ('zero') of the STED beam PSF is still at 1% of the intensity at the donut crest. Hence, for moderate resolution enhancements a 1% central minimum may be acceptable. In the quality function in Figure 2, the red lines display a 500-fold magnification of the function around the STED regime. A 1% central minimum in the STED beam is reached where the magnified function is clipped at the top of the graph (indicating 1 for the non-magnified graph). The width (opening) of the red curve can be used to estimate the wavelength tolerance for the STED beam. The width of the excitation spot is less critical. A quality function level of 0.75 reduces the excitation spot's peak intensity by ~25% and makes it ~10% larger. While the STED beam profile quality largely determines the resolution and dominates the bleaching behaviour, a larger spot is tolerable for the excitation light.

For biomedical multi-colour imaging applications, however, it is desirable to expand the excitation and detection range. In practice, when a dual-colour staining is imaged, for example, with excitation wavelengths of 600 and 650 nm and STED at 775 nm, the shorter-wavelength fluorophore typically has a lower cross-section for stimulated emission and tends to feature slightly lower resolution compared to the longer-wavelength fluorophore. With the conventional easySTED phase plate, acquisition of this colour channel is also compromised by an imperfect excitation PSF (compare Figure 2), which can limit dual-colour imaging. The latter effects make it highly desirable to alleviate this shortcoming of the conventional easySTED phase plates.

We note that also the emission beam will be slightly affected by the chromatic phase plate (Figure 1). Consequently, the overall performance of the easySTED optics is limited in the applicable excitation wavelengths as well as in the detection wavelength range. Improvements in the detection range are especially desirable when imaging densely stained extended samples. A larger range allows to choose smaller detection pinhole sizes and to reject out-of-focus haze with less loss of the signal.[5]

In the following a new phase plate design is presented, which allows to significantly widen the spectral range of chromatic segmented birefringent wave plates for STED. The design also widens the wavelength tolerance at the STED wavelength.

## 2 | MULTIPLE ROTATED RETARDERS ALLOW TO SYNTHESISE A DESIRED SPECTRAL SIGNATURE

The principle for the new design of segmented chromatic easySTED phase plates is based on Pancharatnam's idea to make an achromatic phase plate by stacking phase plates which are rotated relative to each other.[6] This original publication and newer ones such as Saha et al.[7] are focused on providing an optimisation with respect to a wide and flat achromatic design. In our context, it is about a dedicated chromatic design where the optical element shall have different specific retardations across different spectral ranges. We follow the formulation of the problem of

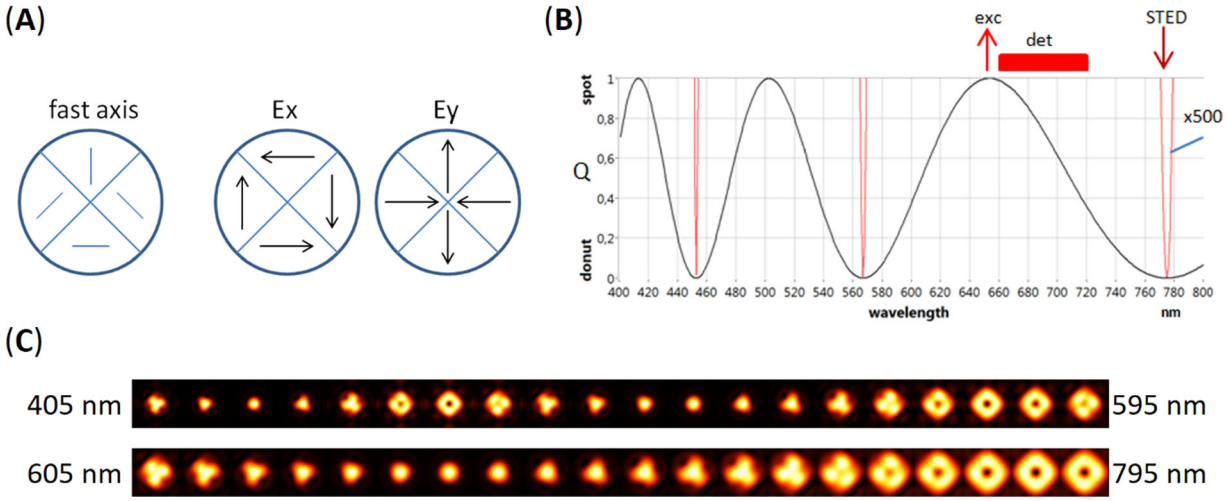


**FIGURE 2** Example of a segmented phase plate with 2.5 $\lambda$ retardation at 775 nm. (A) Segmented phase plate with the fast axes of the retarders. Opposing segments bring about cancelling of polarisations $E_x$ and $E_y$ at the focus position, rendering the STED beam (775 nm) donut-shaped. For the excitation, the retardation is a full wave instead of half-wave, leaving the excitation focal intensity spot-shaped. (B) The quality function, which is 0 at the STED wavelength and 1 at the excitation wavelength. The red curves display a 500-fold magnification. The residual intensity in the donut centre approaches 1% where the red curves are clipped in the graph. (C) The resulting focal intensity distributions (point spread functions) for a fourfold segmented phase plate in 10-nm steps

Saha et al. by writing the behaviour of a stack of optical retarders in the segments as the product of Jones matrices $J_N$. $J_N$ describes a stack of $N$ retarders with $j_i$ being the Jones matrix of a stack element with a rotation angle of $\alpha_i$. The phase shift of $\phi_i$ between the ordinary and extraordinary axis is wavelength- dependent. For the following consideration let the product result in a $2 \times 2$ matrix with elements $A$, $B$, $C$ and $D$, which depend on the wavelength because $\phi_i$ depends on the wavelength

$$J_N = \prod_{i=1}^{N} j_i = \begin{pmatrix} A & B \\ C & D \end{pmatrix} \tag{1}$$

with

$$j_i = \begin{pmatrix} \cos\alpha_i & -\sin\alpha_i \\ \sin\alpha_i & \cos\alpha_i \end{pmatrix} \begin{pmatrix} 1 & 0 \\ 0 & e^{i\phi_i} \end{pmatrix} \begin{pmatrix} \cos\alpha_i & \sin\alpha_i \\ -\sin\alpha_i & \cos\alpha_i \end{pmatrix}. \tag{2}$$

Each of the retarders in the stacks is characterised by the retardation at the design wavelength and its segment rotation angle. In order to produce a donut shape for the STED wavelength, it is required that two opposing segments of the segmented wave plate generate opposite field directions, such that they cancel each other in the focus of the objective. This can be fulfilled for example if the following conditions are met:

1. The stack of retarders acts as a half-wave phase plate at the STED wavelength.
2. Opposing segments are rotated by 90° with respect to each other.
3. Each segment contains the same stack of retarders but is rotated with respect to the other segments.

Condition 2 in general leads to the condition for the STED wavelength:

$$\left| \left( J_N + \begin{pmatrix} 0 & 1 \\ -1 & 0 \end{pmatrix} J_N \begin{pmatrix} 0 & -1 \\ 1 & 0 \end{pmatrix} \right) \vec{E} \right|^2 = \left| \begin{pmatrix} A+D & B-C \\ C-B & A+D \end{pmatrix} \vec{E} \right|^2 = 0. \tag{3}$$

Now let us choose retardations $\phi_i$ of each stack element to be a multiple of $\pi$ at the design wavelength (STED wavelength) and at the same time the total retardation of the whole stack for STED to be

$$\sum \phi_i = \pi \cdot (2n+1). \tag{4}$$

With that choice, all Jones matrices with an even multiple of $\pi$ result in a unity matrix and products consisting of Jones matrices with an odd multiple of $\pi$ are always of the type (5)

$$j = \begin{pmatrix} \cos^2\alpha - \sin^2\alpha & 2\cos\alpha\sin\alpha \\ 2\cos\alpha\sin\alpha & \sin^2\alpha - \cos^2\alpha \end{pmatrix} \tag{5}$$

So, having chosen the $\phi_i$ to be an even or odd multiple of $\pi$ and simultaneously forcing the condition in Equation (4) for the STED wavelength lets us freely choose the

rotation angles in order to shape the wavelength range for the excitation and detection wavelengths, while at the same time the STED donut always remains conserved and Equation (3) is fulfilled for the STED wavelength. At the STED wavelength the stack thus consists of half and full-wave retarders, such that there effectively is an odd number of halfwave retarders present.

Actually, at first glance, it may seem surprising that such a spectral design is possible at all with a single material type. In contrast, achromatic lens designs require different dispersive materials for colour corrections. However, a better understanding may be gained if we rewrite (2) as a sum of two matrices

$$j = F + e^{i\phi}G \tag{6}$$

with

$$F = \begin{pmatrix} \cos^2\alpha & \sin\alpha\cos\alpha \\ \sin\alpha\cos\alpha & \sin^2\alpha \end{pmatrix}$$

and

$$G = \begin{pmatrix} \sin^2\alpha & -\sin\alpha\cos\alpha \\ -\sin\alpha\cos\alpha & \cos^2\alpha \end{pmatrix}.$$

Then the product of the Jones matrices of the stack becomes

$$J_N = \prod_{i=1}^{N} \left(F_i + e^{i\phi_i}G_i\right) = \begin{pmatrix} A & B \\ C & D \end{pmatrix}. \tag{7}$$

If Equation (7) is expanded, we obtain an expression of the general form (8).

$$J_N = a + be^{i\phi_1} + ce^{i\phi_2} + de^{i\phi_3} \cdots + fe^{i(\phi_1+\phi_2)} + ge^{i(\phi_1+\phi_3)} + he^{i(\phi_2+\phi_3)} + \cdots + pe^{i(\phi_1+\phi_2+\phi_3)} + \ldots \tag{8}$$

This actually very much resembles a Fourier series expansion where the coefficients are ultimately defined by the rotation angles of the retarders in the stacks. Note that Equation (8) contains all combinations of sums of $\phi_i$. This suggests why, with a proper selection of the retardation orders of retarders fulfilling (4), many Fourier terms can be present to synthesise a desired spectral signature.

Since the coefficients $(a, b, c, \ldots)$ in the series (8) are coupled in a more or less complex way, an arbitrary function synthesis is not readily possible like in a general Fourier series with freely selectable coefficients. And yet we show in the results below that a number of highly interesting segmented phase plates can be constructed nonetheless. This consideration may also provide a rationale why it is possible at all to influence the spectral behaviour by using a stack of retarders made from a single material type.

Note that the sequence (ordering) of Jones matrices, respectively stack elements, matters. Since the angle of the first element can be set to zero with $N$ retarders, $N - 1$ angles can be chosen in order to tune the spectral signature outside the STED wavelength. Obviously, two subsequent elements in the stack shall not have the same angle nor shall they be orthogonal with respect to each other. Otherwise this pair would correspond to a single element with the sum or difference of the retardation orders of the two elements. This in turn would correspond to a stack with fewer elements. In any case, without further analysis of the coupling of the coefficients, it is readily possible to find good approximations by simulating the spectral retardation of the stack while tuning the angles interactively.

In order to simulate the spectral behaviour, we add the effects of the electric field components of two opposing segments with one of the segments rotated by 90° (Equation 3), which allows to define the quality function

$$Q(\lambda) = \frac{1}{2}\left(|A + D|^2 + |B - C|^2\right) \tag{9}$$

with the wavelength-dependent $A$, $B$, $C$ and $D$ from Equation (1) or (7).

If $Q$ is 0, then a perfect donut is formed, and if it equals 1, a perfect diffraction-limited standard spot is formed. A $Q$ of 2 per mille leads to ca. 1% residual intensity in the centre relative to the crest of the donut. This in turn gives rise to ~50% signal loss at a resolution of around 30 nm in STED imaging. As already mentioned, the excitation is less critical, as a $Q$ of 0.9 gives rise to a peak intensity loss of just about 2%. In practice even a $Q$ of 0.7 is tolerable in most cases.

We have written a Labview program which immediately displays the graph of the quality function while tweaking the phase angles interactively. Searching for a close-to-desired spectral design is manageable interactively in some minutes in case of just a few layers like the ones presented here because of the restricted degrees of freedom. In this, the parameter space (design wavelength, number of elements and their retardations, and individual rotation angles) was explored in small increments and the aim was to obtain profiles with $Q$ close to 1 at the wavelength ranges intended for excitation and emission, and $Q$ close to 0 over a sufficiently broad range around the STED wavelength. Steep edges in $Q$, a kind of step-function behaviour, was considered advantageous. For finer tuning demands, more complex stack compositions may be required as well as numeric optimisation methods.

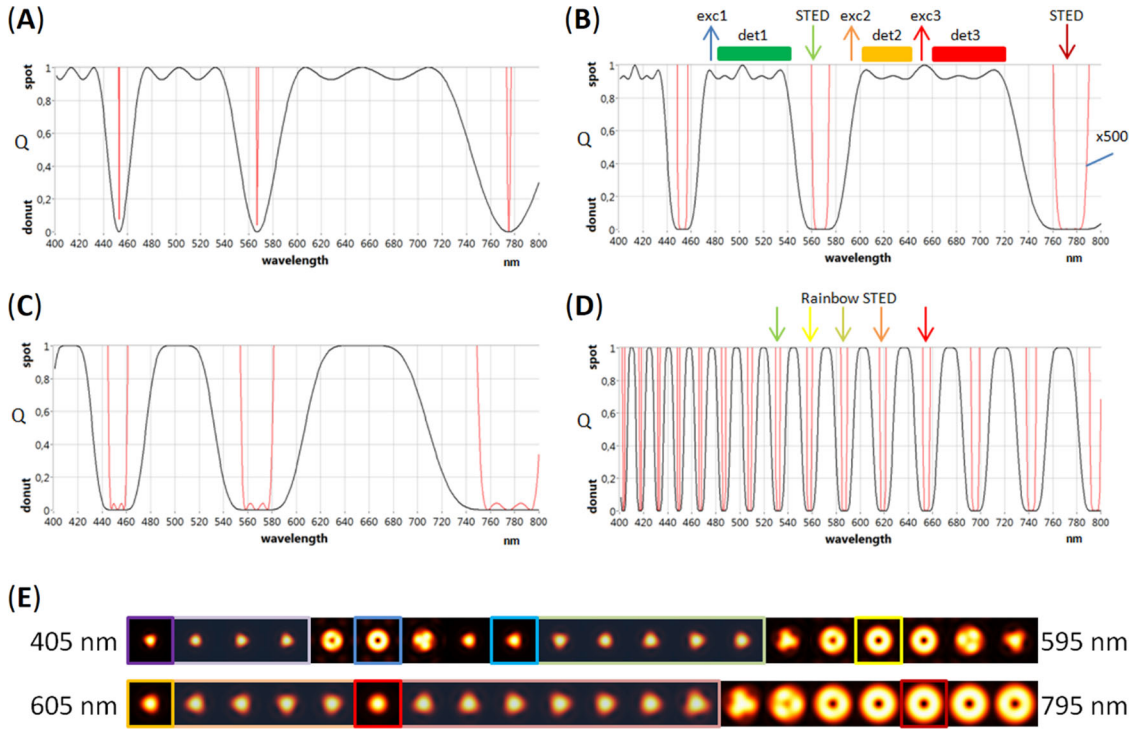


**FIGURE 3** Examples of wavelength-tuned easySTED phase plates. (A) Quality function of a 3-layer design for a wide excitation range with three 2.5 $\lambda$ quartz retarders (at 775 nm) rotated by 45° with respect to each other. (B) Wide-excitation-and-STED-range quality function of a 4-layer design with 2.5 $\lambda$, 7.5 $\lambda$, 10 $\lambda$ and 2.5 $\lambda$ (at 775 nm) quartz retarders with rotation angles of 0°, 35°, −40° and −104°. (C) Low ringing design: quality function with 2.5 $\lambda$, 5 $\lambda$ and 5 $\lambda$ (at 775 nm) quartz retarder with the angles 0°, 51° and −54°. (D) The same design as in (C) but with a design wavelength of 3726 nm and made from MgF. (E) Normalised point spread functions of the phase plate design in (B) in 10 nm steps. Here the point spread functions of a sixfold segmentation are shown, which results in almost perfectly round donut shapes across wide wavelength ranges. The excitation, STED and detection ranges are marked respectively

## 3 | THEORETICAL RESULTS

For comparison of the new designs with multiple rotated retarders see the quality function in Figure 2B for a design with a single retarder in each segment.

In Figure 3, a selection of potentially interesting designs is shown. Figure 3A displays the quality function of a stack of three 2.5 $\lambda$ quartz retarders at 775 nm which are rotated by 45° with respect to each other. Compared to the single retarder design in Figure 2, the acceptable excitation/detection range is expanded to 590–730 nm. But this comes at the price of a narrower STED range which shrunk to approximately ±2 nm. This is very close to the manufacturing tolerances of the phase plates and the wavelength tolerances of the popular 775 nm fibre lasers for STED. It is therefore desirable to also widen the spectral range for the STED laser. Figure 3B shows an example with wide excitation and STED range. The design includes 4 quartz retarders with the orders 2.5 $\lambda$, 7.5 $\lambda$, 10 $\lambda$ and 2.5 $\lambda$ at 775 nm with rotation angles of 0°, 35°, −40° and −104° respectively. Note that the acceptance range for STED is expanded to ∼30 nm, which makes it even useable for broadband pulsed lasers such as the Ti:Saphire laser. At the same time the manufacturing tolerances are relaxed. Shifted a few nanometres towards shorter wavelengths, this design could be used for a dual-channel STED laser system using a 560 nm as well as a 775 nm fibre laser.

The quality function in Figure 3C, showing less ringing, is formed by a three-element phase plate with 2.5 $\lambda$, 5 $\lambda$ and 5 $\lambda$ for 775 nm with the angles 0°, 51° and −54°. With the design wavelength set to 3726 nm we obtain the comb-like structure of the quality function of Figure 3D. This design using MgF fits all stronger lines (654 nm, 618 nm, 587 nm, 558 nm, 532 nm) of a Raman fibre laser.[8] As a result, switching the STED wavelength becomes possible without system re-alignment. A number of excitation ranges are available simultaneously, which may be addressed by a white light laser. Altogether, spectrally very flexible new STED designs become possible especially when the new designs are combined with directional beam splitters[9] instead of spectrally fixed dichroic beam splitters. Optionally even another copy of the wave plate in the detection beam path could recover the spot shape in order to allow for smaller detection pinhole sizes and improved sectioning.[5]

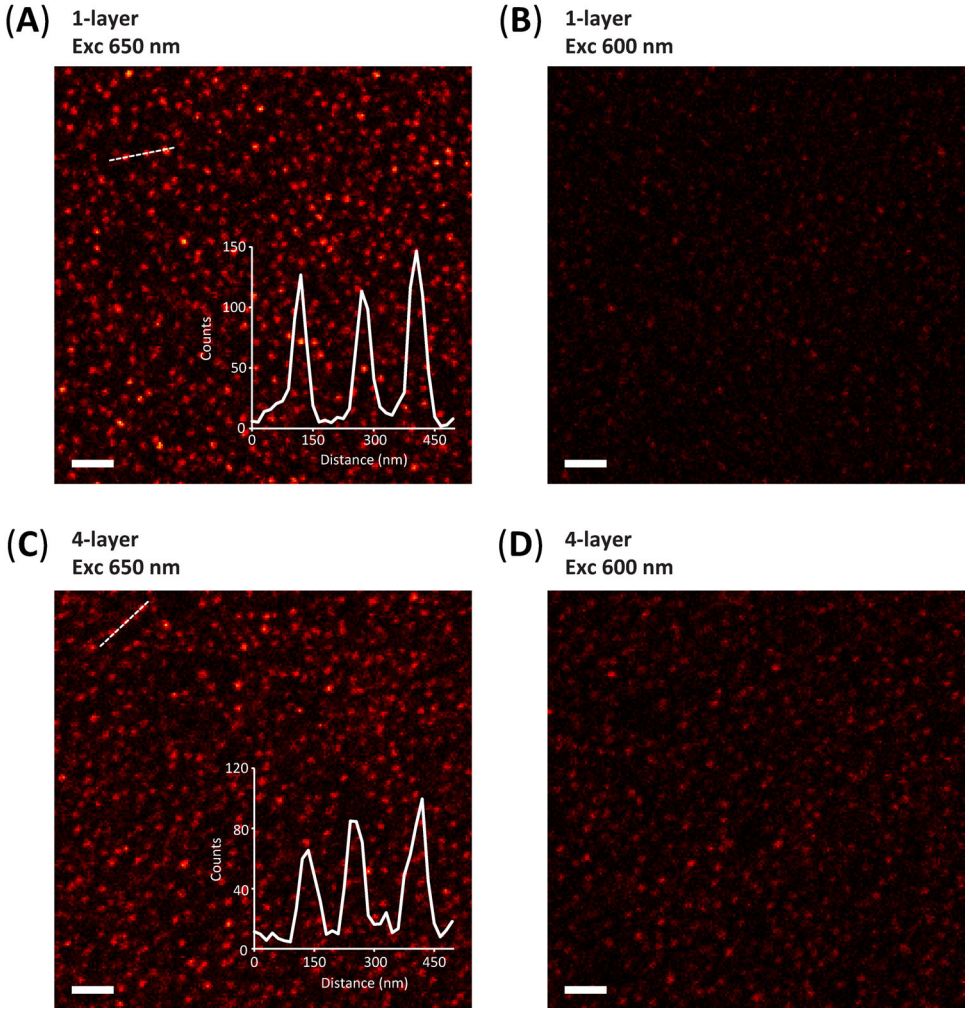


**FIGURE 4** Images of 26 nm Crimson Fluospheres excited at 600 vs. 650 nm with STED at 775 nm. For comparing the intensities, equal look-up table scaling was set in all. (A) Conventional single-layer phase plate at 650 nm excitation. (B) Conventional single-layer phase plate at 600 nm excitation. (C) New 4-layer phase plate at 650 nm excitation. (D) New 4-layer phase plate at 600 nm excitation. As expected, there is no significant difference at 650 nm excitation, whereas at 600 nm excitation, the conventional phase plate gives rise to significantly lower intensities, about twofold lower. Intensity profiles in the shown positions indicate the sub-diffraction resolution. Scale bars: 300 nm

## 4 | PRACTICAL DEMONSTRATIONS

In order to practically verify the calculated designs, we manufactured as an example the easySTED phase plate of Figure 3B with wide excitation and STED range. First a stack of 4 quartz retarders with 2.5 $\lambda$, 7.5 $\lambda$, 10 $\lambda$ and 2.5 $\lambda$ (at 775 nm) at rotation angles of 0°, 35°, −40° and −104° was made. The cemented stack then was cut into 60° pie-shaped segments with axes rotated −30° with respect to each other. The segments were then re-assembled and cemented between two cover plates. The new phase plate replaced the conventional single-layer phase plate in a system as described in Görlitz et al.[9] Fluorescent beads (Figure 4) and cellular samples (Figure 5) served to compare the STED imaging with the two phase plates at the two excitation wavelengths 600 and 650 nm.

In assessing the performance of the plates, we note that from Figure 2B one can expect for the old design that in a two-colour STED experiment with 600 and 650 nm excitation the peak excitation intensity at 600 nm would only be 40% of the respective diffraction-limited spot. For light at 600 nm, most of the power is spilled around the very centre and cycles molecules unnecessarily without benefitting the resulting image. (Simply increasing the excitation laser intensity in order to reach the same fluorescence intensity as a diffraction-limited spot would come at the cost of higher bleaching).

In contrast, with the new 4-layer phase plate of Figure 3B, the excitation is at $Q \approx 90\%$ still almost diffraction-limited and does not cause excessive cycling and bleaching of the molecules. The expectation therefore would be that the old phase plate design will perform approximately half as well as the new design, with respect

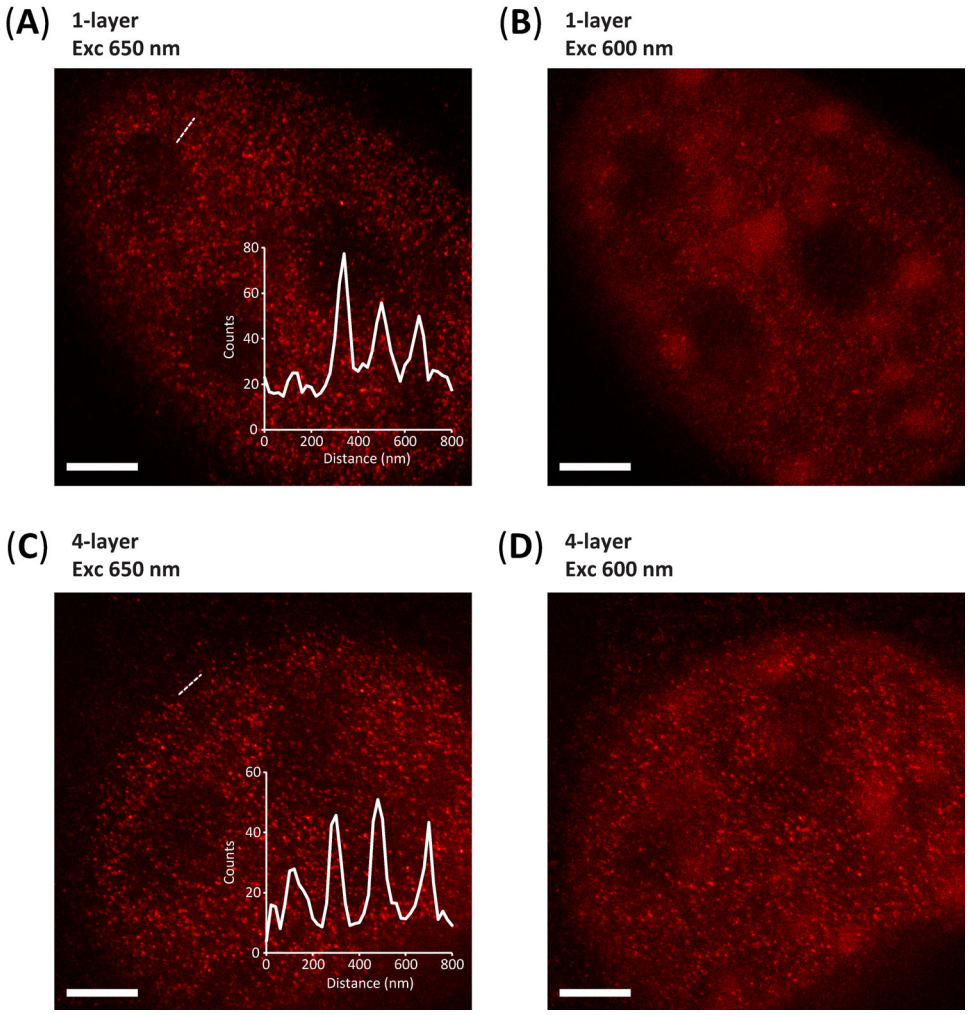


**FIGURE 5** Histones in cells were immunostained simultaneously with Abberior STAR600 and STAR635P. STED images were taken with 600 nm excitation for STAR600 and 650 nm excitation for STAR635 and a common STED wavelength of 775 nm. (A, B) Images taken with the conventional single-retarder easySTED phase plate. (C, D) Images taken with the new 4-layer design with 2.5 $\lambda$, 7.5 $\lambda$, 10 $\lambda$ and 2.5 $\lambda$ (at 775 nm) quartz retarders with rotation angles of 0°, 35°, −40° and −104°. (A, C) STAR635P excited at 650 nm and (B, D) STAR600 excited at 600 nm. As expected from the calculations, the two phase plates do not significantly differ at 650 nm. At an excitation wavelength of 600 nm, a marked improvement in brightness and contrast is observed. Intensity profiles in the shown positions indicate the sub-diffraction resolution. Scale bars: 2 $\mu$m

to image signal intensities. (It is interesting to point out that for perfect, non-bleaching dyes the advantage would not be there. Real dyes bleach, however, especially at shorter wavelengths.) With respect to the resolution, the new phase plate does not perform better, because the resolution only depends on the STED light action. And yet, convincing STED images also depend on the noise content of the image.

The described effect is recognisable by eye in the images (Figure 4). As quantitative fluorescence measurements depend on many factors which are often not sizeable individually, we prefer to compare the *relative* image intensities with 600 and 650 nm excitation, for the new and for the old phase plate design.

To this end, we extracted the background intensity at void regions in the images (Figure 4) and the average intensity in the images. The ratios of the background-subtracted average intensities indicate that the intensity, with 600 nm excitation, for the new phase plates is indeed twice as with the old design. At 650 nm excitation, the intensities with the two plates are comparable.

As a separate comparison of the image intensities, we fitted Gaussian functions to more than 50 individual spots in each of the images. As expected, we found no significant STED resolution differences (full-width-half-maximum values: 30–35 nm) irrespective of the excitation or phase plate type. But the spot brightnesses at 600 nm excitation are found 1.7- fold higher with the new phase

plate compared to the old phase plate, in both cases determined relative to the respective brightnesses at 650 nm excitation. The difference to the average intensity comparison above may be due to the preferred manual selection of brighter spots, and thereby overestimating the brightness in the darker images. A further alternative estimation of the brightnesses by fitting a distribution of Gaussians to the auto-correlations of the full images also results in a factor of 2 improvement of the brightness (new plate to old plate) at 600 nm excitation.

The image data in Figure 5 were not assessed quantitatively, but the lower image brightness and contrast at 600 nm excitation for the old 1-layer design versus the new 4-layer design is apparent.

## 5 | DISCUSSION AND CONCLUSIONS

The easySTED principle allows for rugged and virtually alignment-free STED microscope setups. The principle requires chromatic phase plates to form the STED beam into a donut while the excitation wavelengths remain focused as standard spots. Early chromatic designs were rather limited in the choice of the spectral characteristics. This paper has shown that chromatic segmented easySTED phase plates with wide excitation and STED ranges can in fact be designed and manufactured with available standard methods for improved multi-colour imaging and multiple STED wavelengths. The design of a wider STED range actually relaxes the tolerances for the laser wavelengths as well as for manufacturing the retarders. Additionally, this allows the use of TiSa lasers which exhibit a wider spectral bandwidth.

All retarders discussed, with the exception of Figure 3D (which is designed for MgF), are made from quartz which is very commonly used for optical retarders and can be manufactured with a retardation tolerance of 1–2 nm and a rotation tolerance of 1°, causing little-noticed performance changes. The assembly process of the new wave plates with stacks of retarders does not differ much from the conventional ones from Reuss et al.,[2] only in that the retarders are cemented into the stack before the ca. 1 mm thick stack is cut into segments as in the previous designs.

The STED images of technical as well as biological samples show a marked improvement of the signal at the shorter wavelengths where the conventional phase plates are subject to significant compromise with respect to the excitation PSF. This underscores the advantage of the new design, especially for multi-colour imaging of critical biological samples, enabling further technical progress in fluorescence nanoscopy.[10]

It should be mentioned here that, of course, also mixtures of different materials such as Quartz, MgF, and other birefringent crystals, or including achromatic elements in the stacks, lead to a larger number of special solutions. For clarity in demonstrating the principles only examples consisting of a single crystal type are shown here. The use of a single material type in a stack and the consideration of the product of Jones matrices as Fourier series drastically reduce the parameter space. On the one hand, a large number of other potential approximations for the desired spectral design are disregarded here at will, but on the other hand this allows for an easy interactive search and finding many designs that well approximate the desired spectral signature for several laser combinations by simulation. It goes without saying that the described method is not restricted to STED microscopy but also applicable to other RESOLFT methods[1] or optical instrumentation requiring retarders with dedicated spectral polarisation control.

## ACKNOWLEDGMENTS

We thank the optics workshop of the Max Planck Institute for Biophysical Chemistry (now: MPI for Multidisciplinary Sciences), Göttingen, for manufacturing and assembling the phase plates.

On the occasion of this Festschrift, we wish to send congratulations and warm greetings to our esteemed colleague Tony Wilson. For one of us (S.W.H.), Tony's pioneering work in confocal microscopy and interactions in his Oxford laboratory have been a major source of inspiration and motivation for joining the field of optical microscopy.

## ORCID

*Beatrice Ellerhoff* https://orcid.org/0000-0002-3200-8280
*Steffen J. Sahl* https://orcid.org/0000-0003-2917-0778
*Stefan W. Hell* https://orcid.org/0000-0002-9638-5077

## REFERENCES

1. Hell, S. W. (2015). Nobel lecture: Nanoscopy with freely propagating light. *Reviews of Modern Physics*, *87*, 1169–1181.
2. Reuss, M., Engelhardt, J., & Hell, S. W. (2010). Birefringent device converts a standard scanning microscope into a STED microscope that also maps molecular orientation. *Optics Express*, *18*, 1049–1058.
3. Wildanger, D., Bückers, J., Westphal, V., Hell, S. W., & Kastrup, L. (2009). A STED microscope aligned by design. *Optics Express*, *17*, 16100–16110.
4. Richards, B., & Wolf, E. (1959). Electromagnetic diffraction in optical systems II. Structure of the image field in an aplanatic system. *Proceedings of the Royal Society of London A*, *253*, 358–379.
5. Wilson, T. (2011). Resolution and optical sectioning in the confocal microscope. *Journal of Microscopy*, *244*(Pt 2 2011), 113–121.
6. Pancharatnam, S. (1955). Achromatic combinations of birefringent plates. *Proceedings of the Indian Academy of Sciences XLI(4), Section A*, *137*.

7. Saha, A., Chakraborty, S., & Bhattacharya, K. (2014). Achromatic half-wave combination of birefringent plates. *Optik*, *125*, 4534–4537.
8. Rankin, B. R., & Hell, S. W. (2009). STED microscopy with a MHz pulsed stimulated-Raman-scattering source. *Optics Express*, *17*, 15679–15684.
9. Görlitz, F., Hoyer, P., Falk, H. J., Kastrup, L., Engelhardt, J., & Hell, S. W. (2014). A STED microscope designed for routine biomedical applications. *Progress in Electromagnetics Research*, *147*, 57–68.
10. Sahl, S. J., Hell, S. W., & Jakobs, S. (2017). Fluorescence nanoscopy in cell biology. *Nature Reviews Molecular Cell Biology*, *18*, 685–701.

**How to cite this article:** Engelhardt, J., Ellerhoff, B., Gürth, C.-M., Sahl, S. J., & Hell, S. W. (2022). Designing chromatic optical retarder stacks for segmented next-generation easySTED phase plates. *Journal of Microscopy*, 1–9.
https://doi.org/10.1111/jmi.13143